J Fluoresc (2014) 24:473–480
DOI 10.1007/s10895-013-1316-5

ORIGINAL PAPER

A Novel Ratiometric Fluorescent Mercury Probe Based on Deprotonation-ICT Mechanism

Puhui Xie · Fengqi Guo · Sen Yang · Denghui Yao · Guoyu Yang · Lixia Xie

Received: 1 September 2013 / Accepted: 9 October 2013 / Published online: 15 October 2013

Abstract A new NBD-rhodamine dye (**1**) was developed as a colorimetric and ratiometric fluorescent chemosensor for Hg^{2+} with good selectivity in aqueous ethanol solutions under neutral to basic conditions. Sensor **1** showed absorption at 468 nm and a weak emission at 529 nm (ϕ_F=0.063) in ethanol/aqueous tris buffer (9:1, v/v) of pH 9.17 solution. Bathochromic shifts in both absorption (492 nm) and fluorescence spectra (569 nm, ϕ_F=0.129), respectively upon addition of 2 equiv. of Hg^{2+} were observed. The ring-opening reaction of the spirolactam form to the corresponding xanthene form was not found. The interaction of Hg^{2+} with chemosensor **1** resulted in the deprotonation of the secondary amine conjugated to the NBD component so that the electron-donating ability of the N atom was enhanced. Deprotonation-ICT mechanism of secondary amines was suggested for the ratiometric fluorescent chemosensing for Hg^{2+}.

Keywords Chemosensor · Hg^{2+} · Ratiometric sensing · Fluorescent sensing · Deprotonation-ICT · NBD-rhodamine dye

Introduction

Mercury is one of the most prevalent toxic metals in the environment and gets to the body orally or dermally [1, 2]. The extreme toxicity of mercury and its derivates results from its high affinity for thiol groups in proteins and enzymes, leading to the dysfunction of cells and causing health problems [3, 4]. Therefore, exploration of selective and efficient methods for the monitoring of mercury has emerged as a significant goal in the area of chemical sensors in recent years. Fluorogenic methods in conjunction with suitable probes have become the preferable means for detecting trace amounts of species such as metal ions because fluorimetry is rapidly performed, is nondestructive, and is highly sensitive [5, 6]. The most reported fluorescent sensors display an increase or decrease in the emission intensity upon binding to analytes of interest.

As the change in fluorescence intensity is the only detection signal, factors such as instrumental efficiency, environmental conditions, and the probe concentration can interfere with the signal output. To eliminate these effects, a ratiometric fluorescent measurement is desirable [7, 8]. This technique uses the ratio of the fluorescent intensities at two different wavelengths, and provides a built-in correction for environmental effects, and stability under illumination, allowing precise and quantitative analysis and imaging even in complicated systems. Therefore, a sensor displaying a ratiometric response for Hg^{2+} quantitative detection is required to reduce the interference ascribed to deviations in detecting parameters and microenvironments. Different approaches have been proposed to realize ratiometric Hg^{2+} sensing and overcome the emission quenching nature of Hg^{2+} [9–14]. Spirocyclic derivatives of rhodamine are useful sensing platforms due to the ring-opening process leading to "turn-on" fluorescence change. A spirolactam ring exists in the "ring-closed" state without cations and is completely nonfluorescent. Addition of suitable cations leads to ring opening, which results in significant fluorescence enhancement. A fluorescence resonance energy transfer (FRET) based ratiometric sensor for Hg^{2+} detection was successfully developed, in which a NBD

Electronic supplementary material The online version of this article (doi:10.1007/s10895-013-1316-5) contains supplementary material, which is available to authorized users.

P. Xie (✉) · S. Yang · G. Yang · L. Xie
College of Sciences, Henan Agricultural University, Zhengzhou 450002, People's Republic of China
e-mail: phxie2013@163.com

F. Guo (✉) · D. Yao
College of Chemistry and Molecular Engineering, Zhengzhou University, Zhengzhou 450001, People's Republic of China
e-mail: fqguo@zzu.edu.cn

derivative was covalently confined into a thin layer of silica nanoparticles as the donor; and a spirolactam rhodamine derivative (SRhB) was covalently linked onto the particle surface as the mercury ion probe. The presence of Hg^{2+} can trigger an efficient ring-opening reaction of the spirolactam rhodamine, affording efficient FRET-based ratiometric detection for mercury ions in water [15, 16].

Fluorescent chemosensors that show a shift in emission upon binding with analytes are particularly attractive because they are not only capable of ratiometric sensing of analytes, but also offer advantages over conventional monitoring of fluorescence intensity at a single wavelength [17]. The internal charge transfer (ICT) mechanism is widely exploited for ion sensing because of the advantages of spectral shifts and quantitative detection [18, 19]. When a fluorophore contains an electron-donating group (often an amino group) conjugating to a fluorophore, it undergoes ICT from the donor to the fluorophore upon light excitation. If a cation promotes the electron-donating character of the electron-donating group, the absorption and fluorescence spectra should be red-shifted. Conversely, if the electron-donating character of the electron-donating group is reduced, blue shifts of both the absorption and fluorescence spectra are expected. However, the selective fluorogenic detection of mercury ions has always been hard due to its closed-shell d^{10} electronic configurations which cause them to be spectroscopically silent [20, 21]. Reports of the ratiometric fluorescence probes for Hg^{2+} based on ICT are considerably limited.

Herein, we report a new receptor **1** (Scheme 1) based on a nitrobenzoxadiazolyl (NBD) liked with a spirolactam rhodamine derivative by diethylenetriamine. The NBD fluorophore in **1** exhibited the intramolecular push−pull electronic effect, possessing a condensed furazan ring (orange-red color) [22, 23]. Its absorption and fluorescent spectra are expected to change, upon the interaction with analytes. This fluorophore was selected on the basis of its optimal wavelength of excitation/emission being compatible with currently available spectrofluorometers and its minimal self-quenching and photobleaching [24, 25]. The NBD - spirolactam rhodamine dye shows high selectivity for Hg^{2+} over other possible competitive cations based on deprotonation-ICT mechanisms instead of ring-open mechanisms.

Experimental

Reagents and Apparatus

Deionized water (distilled) was used throughout the experiment as solvents. All the chemicals of analytical grade for syntheses were purchased from commercial suppliers and were used without further purification. The stock solutions of metal ions (5 mM) were prepared in deionized water from their chloride salts of Cr^{3+}, Fe^{3+}, Co^{2+}, Ni^{2+}, Hg^{2+} and Cu^{2+} and nitrate salts of Pb^{2+}, Cd^{2+}, Ag^{+}, Mn^{2+}, Zn^{2+} and Hg^{2+} of analytical grade. Stock solution of **1** (1 mM) was prepared in acetonitrile. Tris–HCl buffer solutions were prepared using proper amount of Tris and HCl under adjustment by a pH meter. Ethanol and 2 mM tris–HCl buffer aqueous solutions with certain volume ratio are mixed for pH investigation and sensing experiments.

^{1}H NMR and ^{13}C NMR spectra of **1** were recorded with a 400 MHz Varian spectrometer. Electrospray ionization mass spectra (ESI-MS) were measured on a micrOTOF-Q II system. Elemental analyses were carried on a Flash EA 1112 elemental analyzer. Absorption spectra were obtained on a TU1901 Ultraviolet–visible spectrophotometer. The fluorescence spectra were measured with a Cary Eclipse fluorescence spectrometer. For fluorescence quantum yield (ϕ_F) measurements, the absorbances at the excitation wavelengths were kept below 0.1. Quinine sulphate (ϕ_F=0.55) in 0.1 M sulphuric acid [26] was used as standards. The pH values were measured with a pH S-3C pH meter.

Syntheses

As shown in Scheme 1, compound **1** was synthesized similar to the published procedure by reacting compound **2** with 4-chloro-7-nitro-1,2,3-benzoxadiazole (NBD-Cl) in dichloromethane [27].

Synthesis of **2**

Compound **2** was prepared similar to the reported procedures by using rhodamine B and diethylenetriamine as starting materials [28]. Diethylenetriamine (5 ml, 47 mmol) was added into rhodamine B (1.245 g, 2.6 mmol)in 30 ml absolute ethanol. The mixture was refluxed for 20 h. The reaction mixture was allowed to cool to room temperature and the solvent was removed using a rotary evaporator. CH_2Cl_2 (100 ml) and H_2O (100 ml) were added to the residue. The organic layer was washed with H_2O (50 ml) twice and dried over anhydrous Na_2SO_4 and filtered. The solvent was removed under reduced pressure. **2 (** 1.22 g, 89 %) was collected as a light brown solid. Mp: 156–157 °C. Anal. Calcd. for C32H41N5O2: C, 72.83; H, 7.83; N, 13.27. Found: C, 72.60; H, 7.89; N, 13.17 %.

Synthesis of **1**

Compound **2** (0.42 g, 0.78 mmol) was dissolved in 20 ml CH_2Cl_2, followed by addition of NBD-Cl (0.158 g, 0.79 mmol) and 5 drops of NEt_3. The mixture was stirred for 12 h at room temperature. The solvent was removed under reduced pressure. And the residue was purified by silica gel column chromatography using ethyl acetate:

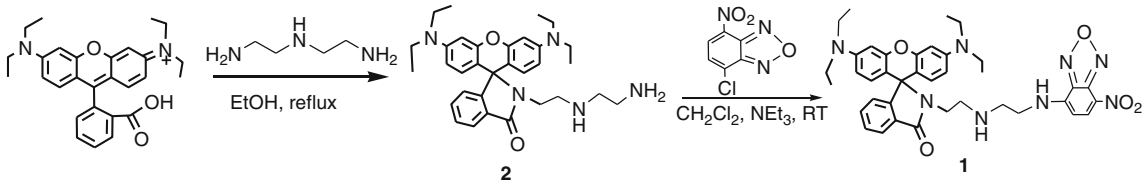

Scheme 1 The synthesis route of **1**

petroleum ether = 1:1 as the eluents to afford the product. Yield: 347 mg (74 %). Mp: 194–195 °C. ^{1}H NMR ($CDCl_3$, δ, ppm), 8.48 (d, J= 8.4 Hz, 1H), 8.01–7.99 (m, 1H), 7.53–7.47 (m, 2H), 7.13–7.11 (m, 1H), 6.46 (d, J= 8.8 Hz, 2H), 6.39 (d, J= 2.4 Hz, 2H), 6.29–6.26 (m, 2H), 6.12 (s, 1H), 3.41 (s, br, 2H), 3.36–3.31 (m, 12H), 2.96 (t, J= 5.6 Hz, 2H), 2.43 (t, J=5.2 Hz, 2H), 1.17 (t, J= 7.2 Hz, 12H) (Fig. S1, Supplementary material). ^{13}C NMR ($CDCl_3$, δ, ppm) 169.26, 153.39, 148.87, 144.25, 136.51, 132.69, 130.99, 128.72, 128.28, 123.84, 123.01, 108.11, 105.45, 97.72, 65.25, 47.58, 44.36, 39.32, 12.57 (Fig. S2, Supplementary material). EI-ms for $C_{38}H_{42}N_8O_5$: 690.33, found: $[M+1]^+$: 691.3, $[M+Na]^+$: 713.2 (Fig. S3, Supplementary material). Anal. Calcd. for $C_{38}H_{42}N_8O_5$: C, 66.07; H, 6.13; N, 16.22. Found: C, 65.77; H, 6.17; N, 16.13.

Results and Discussion

Syntheses

Compound **2** was synthesized through condensation of diethylenetriamine with rhodamine-B in ethanol. Compound **1** was prepared by the aliphatic nucleophilic substitution reaction of **2** with NBD-Cl in high yield (Scheme 1). It was characterized by ^{1}H, ^{13}C NMR and ESI-MS spectroscopies. The characteristic peak of the spiro-carbon of **1** near 65.3 ppm in the ^{13}C NMR spectrum indicates that **1** is predominantly in the form of spirolactam [29]. The nitrogens in the diethylenetriamine linker and the carbonyl oxygen can provide binding unit for Hg^{2+}. The Hg^{2+} binding may affect ICT of the NBD component or ring-opening reaction of the spirolactam form and convert the ligand to the corresponding xanthene form, and consequently induce different spectral change.

The Effect of pH on the Performance of Probe **1**

The pH value of the environment around the fluorescent probe usually shows an effect on its performance toward target metal ions due to the protonation or deprotonation reaction of the fluorophore and the hydrolysis reaction of the metal ions. The fluorescence of **1** at 529 nm upon excitation at 468 nm changed little between pH 10 and 7, and then gradually increased from pH 7 to 2.6. Its pK_a value was 3.5 by sigmoidal fitting (Fig. 1). Below pH 2.6, a shoulder at 580 nm appears due to the ring opened process of the spirolactam of rhodamine component in **1** by H^+ (Fig. S4, Supplementary material). Typically **1** is fluorescent showing an emission band at 523 nm with a fluorescence quantum yield of ϕ_F=0.302 at pH=2.60. When pH was increased, a drastic quenching of fluorescence and a bathochromic shift were observed; in particular, the emission band moves to 527 nm (ϕ_F=0.075) at pH=6.92 and to 532 nm (ϕ_F=0.056) at pH=10.13. This is the typical behavior of chemosensors based on a photo-induced electron transfer (PET) mechanism of the NBD component [30]. The absorption spectra of **1** on variation in pH in acidic solutions showed only small changes in their λ_{max} values with ~15 nm hypsochromic shift. The 468 nm absorption band showed larger changes in absorbance in acidic solutions than in basic solutions. The absorbance gradually increased with increasing the pH from 2.6 to 7.0, and then became almost constant between pH 7.0 and 9.17. At pH 11.11, there was a large change in the absorption shape and band (Fig. S5, Supplementary material). The effects of pH on the deprotonation of **1** induced by Hg^{2+} were investigated by means of the absorption and fluorescence measurements. As the high concentration of Hg^{2+} might cause precipitation of HgO in the alkaline condition, so these experiments were carried out at a pH range from 2.60 to 11.11, with the concentration of **1** fixed at 20 μM and of Hg^{2+} at 24 μM, respectively. In the presence of Hg^{2+}, the absorbance

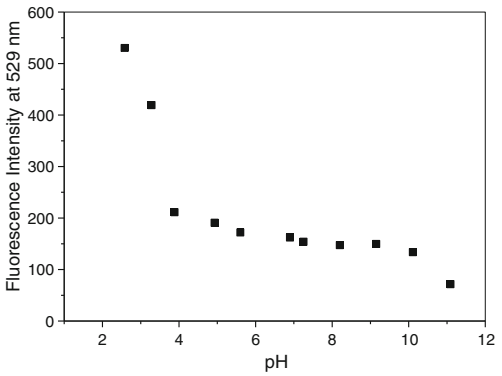

Fig. 1 Influence of pH on the fluorescence intensity at 529 nm of **1** (20 μM) in ethanol–H_2O (9:1, v/v). Excitation wavelength is 468 nm. Ex slit was set at 5 nm. Em slit was set at 10 nm

of **1** at 468 nm steadily increased from pH 2.6 to 3.92 and a longer absorption band at 492 nm developed on increasing the pH of the solution. The absorption at 468 nm reached its limiting value between pH 3.92 and 7.27. Then it began to decrease at pH >7.27. The absorbance of **1** at 492 nm increased with the increasing of pH all the time (Fig. 2a). The absorption spectra in presence of $HgCl_2$ changed greatly at pH 7~10 (Fig. S6). This response may be due to the complexation of the deprotonated N^- with Hg^{2+}.

Due to the protonation of compound **1**, its binding capability with the metal ions is very low in acidic environments. But in the neutral and basic conditions with the increase of pH, the fluorescence peaks are red-shifted gradually with a slight increase in intensity in presence of $HgCl_2$ (Fig. 2b and Fig. S7, Supplementary material). The ratio of the fluorescence intensity (I_{569}/I_{529}) is very low (<0.6) and maintains constant at pH<5 before and after addition of Hg^{2+}. In a wide physiological range of pH from 5.0 to 10.13, I_{569}/I_{529} increases gradually in the presence of Hg^{2+}. At pH 10.13, the emission intensity ratio reaches its maximum value of 3.12 (Fig. S8, Supplementary material). Sensors based on electron donor/acceptor are usually disturbed by proton in the detection of metal ions. Taking into consideration the sensitivity and possibility of precipitation of HgO, a Tris–HCl buffer solution at pH 9.17 was chosen as optimum experimental condition in sensing of $HgCl_2$.

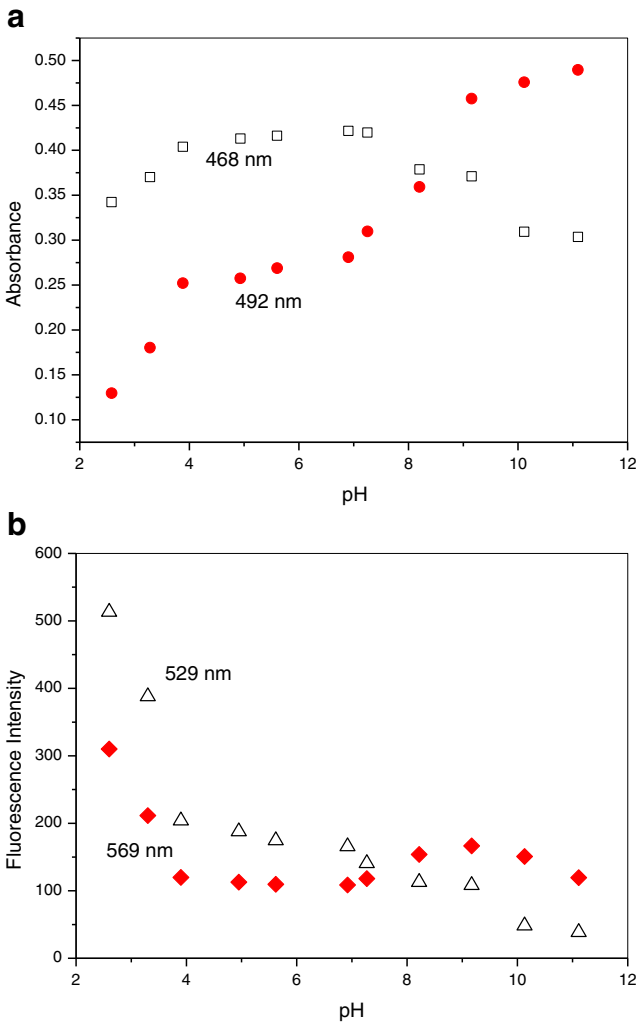

Fig. 2 **a** Dependence of the absorbance at 468 nm (*white square*) and 492 nm (*red circle*) on pH for a solution of **1** (20 μM) in the presence of Hg^{2+} (24 μM) in ethanol–H_2O (9:1, v/v). **b** Dependence of the fluorescence intensity of the band centered at 529 nm (*white triangle*) and 569 nm (*red diamond*) on pH for a solution of **1** (20 μM) in the presence of Hg^{2+} (24 μM) in ethanol–H_2O (9:1, v/v). Excitation wavelength is 468 nm. Ex slit was set at 5 nm. Em slit was set at 10 nm

UV–vis Titration Investigation

The *UV–vis* spectrum of **1** showed the absorption maximum at 468 nm and a π-π* transition at 320 nm in ethanol/aqueous tris buffer (9:1, v/v) of pH 9.17. The lower energy absorption band is attributed to the intramolecular charge transfer transition [31, 32] from the donor N atom of **1** to the acceptor nitrogroup of the NBD moiety. Upon addition of Hg^{2+}, the absorbance at 468 nm decreased gradually and was red-shifted until a new absorption peak at 492 nm appeared and increased with an obvious absorption shoulder at 530 nm. Meanwhile, the absorption band at 320 nm decreased and a new peak at 370 nm appeared and increased. Three isosbetic points at 343 nm, 407 nm and 476 nm appeared in the *UV–vis* spectra (Fig. 3a). Therefore, upon mercury binding there was a 24 nm red-shift in the visible absorption spectral region. The pale yellow solution of **1** in ethanol/aqueous tris buffer (9:1, v/v) of pH 9.17 turned to a red color on addition of Hg^{2+}. Similar absorption spectral responses of **1** to $HgCl_2$ can also be found in neutral conditions without any buffer solutions (Figs. S9, Supplementary material). These characteristics illustrated the transformation from free **1** to the **1**-Hg^{2+} complexes. However, there were no absorption peaks at around 560 nm, which indicated that the spirolactam rhodamine component was not ring-opened by the interaction of Hg^{2+}. The curve established by plotting the ratio of the absorbance at 492 nm and 468 nm (A_{492}/A_{468}) versus mercury ion concentration is shown in Fig. 3b. The absorbance ratio A_{492}/A_{468} increased linearly with the increasing of the Hg^{2+} concentration in the range of 8×10^{-7}~8×10^{-6} mol/L (insert in Fig. 3b). Then the ratio increased slightly with the increase of the concentration of Hg^{2+}. The relationship between the ratio of the absorbance and Hg^{2+} concentration was: $A_{492}/A_{468}=3.90\times10^5C+0.6715$, with a correlation coefficient of $R=0.992$, where C was the concentration of Hg^{2+} in mol/L. The detection limit, based on the definition by IUPAC was found to be 2.4×10^{-7} mol/L from 11 blank solutions. In order to be confirmed with the reversible nature of the complexation, absorption spectra of the mercury complexes of **1** in ethanol/aqueous tris buffer (9:1, v/v) of pH 9.17 were observed upon addition

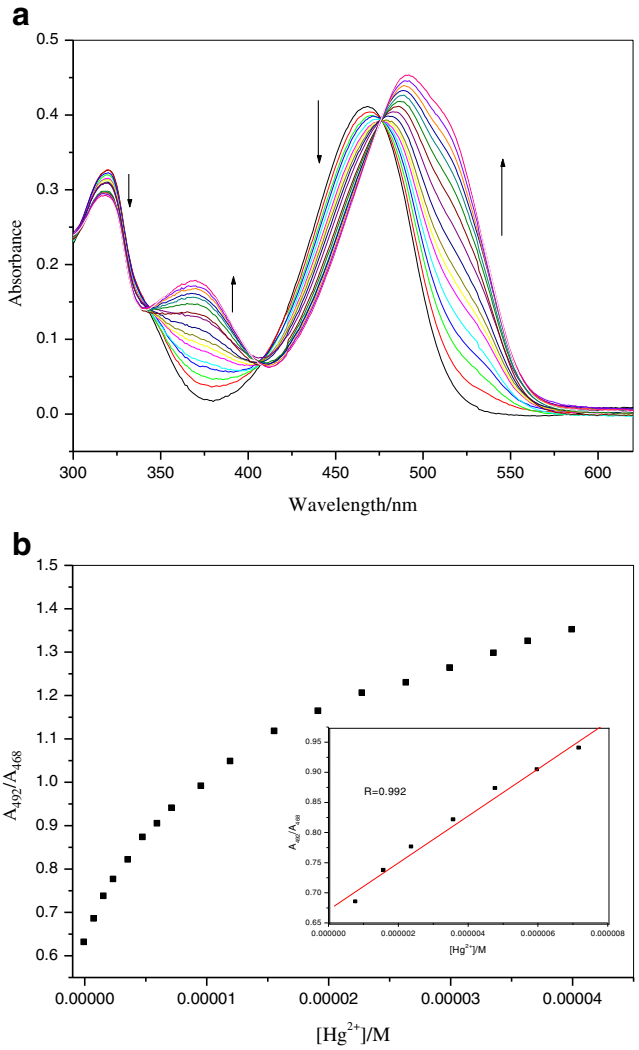

Fig. 3 **a** Absorption spectra of **1** (2×10^{-5} M) in the presence of increasing concentrations of $HgCl_2$ in ethanol/aqueous tris buffer (9:1, v/v) of pH 9.17. **b** Absorbance ratio changes A_{492}/A_{468} of **1** upon gradual addition of Hg^{2+}, inset: A_{492}/A_{468} vs. Hg^{2+} in the concentration range of $0\sim5\times10^{-6}$ M

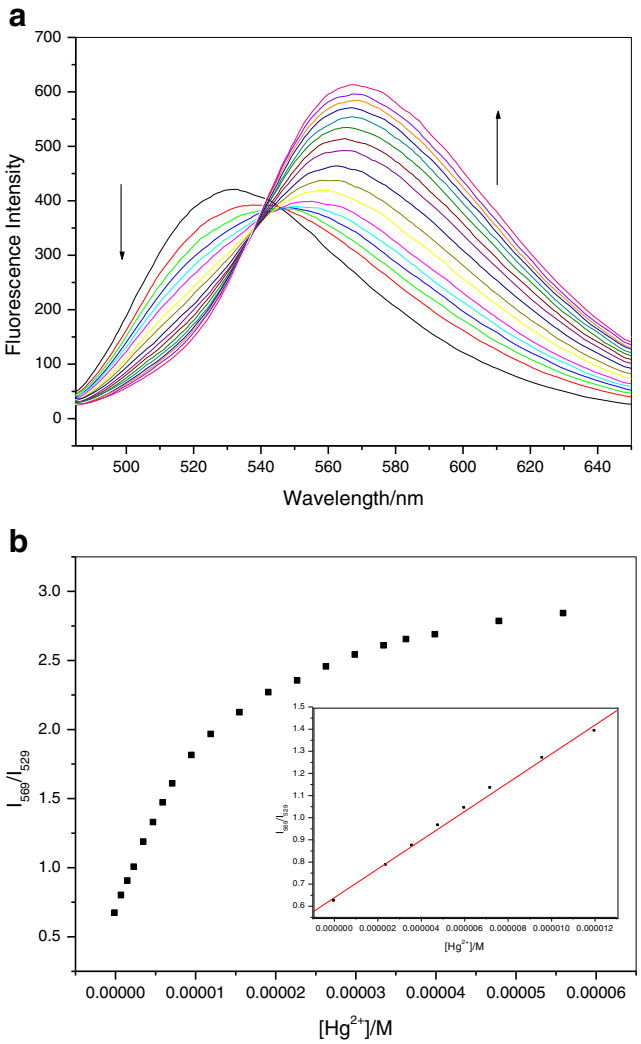

Fig. 4 **a** Fluorescence spectra of **1** (2×10^{-5} M) in the presence of increasing concentrations of $HgCl_2$ ($0\sim5.6\times10^{-5}$ M) in ethanol/aqueous tris buffer (9:1, v/v) of pH 9.17. Excitation wavelength is 468 nm. Both ex slit and em slit were set at 10 nm. **b** Fluorescence intensity ratio changes ((I_{569}/I_{529}) of **1** upon gradual addition of Hg^{2+}

of EDTA. Addition of EDTA resulted in the reverse change in the absorption spectra (Fig. S10, Supplementary material), indicating of a reversible coordination between **1** and Hg^{2+}.

Fluorescence Titration Investigation

The fluorescence changes of **1** upon gradual addition of $HgCl_2$ in ethanol/aqueous tris buffer (9:1, v/v) of pH 9.17 were measured. When excited at its excitation maximum of 468 nm, **1** showed one characteristic fluorescence band centered at 529 nm, which is the typical fluorescence of the NBD fluorophore. $HgCl_2$ titration demonstrated an obvious emission decrease of the band centered at 529 nm (ϕ_F=0.063), with a 40 nm red-shifted to 569 nm. The fluorescence intensity

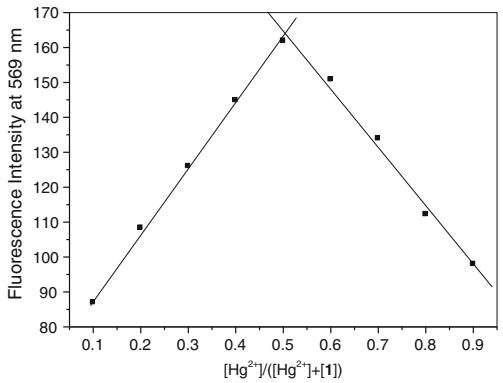

Fig. 5 Job's plot for determining the stoichiometry of **1** and $Hg(NO_3)_2$ in ethanol/aqueous tris buffer (9:1, v/v) of pH 9.17 with a total concentration of 4×10^{-5} M. Excitation wavelength is 468 nm. Ex slit was set at 5 nm. Em slit was set at 10 nm

Scheme 2 Possible recognition mechanism of 1 for Hg^{2+}

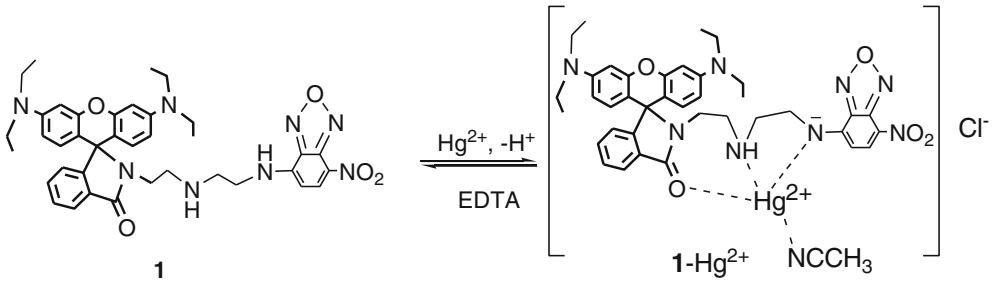

at 569 nm was gradually increased with the titration of $HgCl_2$ (Fig. 4a). The fluorescence quantum yield of 0.129 (2-fold in ϕ_F) at 569 nm when the concentration of $HgCl_2$ was 4×10^{-5} M. An isoemission point appears at near 546 nm at low concentration of $HgCl_2$ (0~10 μM), and another isoemission point appears at near 538 nm at high concentration of $HgCl_2$. Figure 4b shows the dependence of emission intensity ratios at 569 and 529 nm (I_{569}/I_{529}) on the concentration of Hg^{2+}. The emission intensity ratios I_{569}/I_{529} changed from 0.78 to 2.34 when 2 equivalents of Hg^{2+} were added. I_{569}/I_{529} increased linearly with increasing of the Hg^{2+} concentration in the range of 4.4×10^{-7}~ 1.32×10^{-5} mol/L (inset in Fig. 4b). Then the ratio increased slightly with the increase in the concentration of Hg^{2+}. The relationship between I_{569}/I_{529} and Hg^{2+} concentration was: $I_{569}/I_{529}=0.6386+64991C_{Hg}^{2+}$ ($R=0.9975$). The detection limit obtained for Hg^{2+}, estimated by 3σ/k (where σ is the standard deviation of 11 measurements of the blank and k is the slope of the calibration line) was 2.3×10^{-7} mol/L [33, 34]. The fluorescence response of **1** to $HgCl_2$ can also be found in neutral conditions (Figs. S9 and S11, Supplementary material).

Job's plot analysis of the fluorescence titrations with a total concentration of 4×10^{-5} M at 569 nm revealed a maximum at about 0.5 mole fraction (Fig. 5), indicating 1:1 binding stoichiometry. The association constant was calculated to be 1.15×10^{5} M^{-1} according to the *UV–vis* titration profile (Figure S12, Supplementary material).

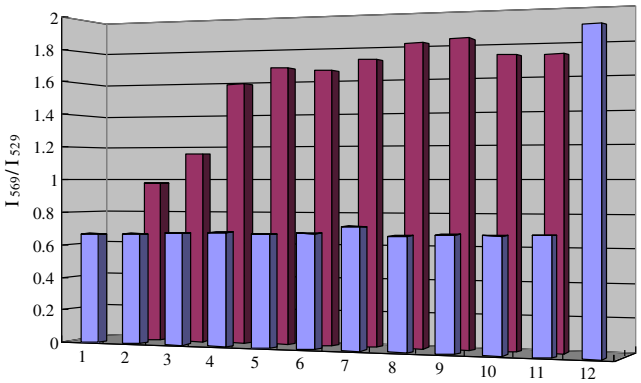

Fig. 6 Selectivity of **1** (20 μM) for Hg^{2+} in the presence of other metal ions (40 μM) in ethanol/aqueous tris buffer (9:1, v/v) of pH 9.17, purple bars represent 1: blank, 2: Cr^{3+}, 3: Fe^{3+}, 4: Cu^{2+}, 5: Pb^{2+}, 6: Zn^{2+}, 7: Cd^{2+}, 8: Ag^{+}, 9: Mn^{2+}, 10: Co^{2+}, 11: Ni^{2+}, 12: Hg^{2+}. *Red bars* represent the subsequent addition of $HgCl_2$ (40 μM) to the solution. The excitation wavelength was 468 nm. Ex slit was set at 5 nm. Em slit was set at 10 nm

Possible Mechanism

The red shifts in both emission and absorption maxima of probe **1** after binding with Hg^{2+} ions can be explained in terms of the possible ICT mechanism [31, 32, 35]. The strong electron-withdrawing effect of the nitrobenzoxadiazolyl (NBD) fluorophore would greatly decrease the electron density on the nitrogen on the ethylenediamine linker, resulting in easier deprotonation of the N-H. The capture of Hg^{2+} ion by **1** is proposed to result in the deprotonation of -NH- conjugated to NBD so that the electron–donating ability of the N atom would be enhanced. As a consequence of this interaction the emission intensity at 569 nm gradually increases. The proposed binding mechanism of Hg^{2+} with **1** was shown in Scheme 2. The interaction between Hg^{2+} and carbonyl oxygen of the rhodamine component in **1** was possibly too weak to be able to induce the ring-opening reaction of the spirolactam form and convert the ligand to the corresponding xanthene form, possibly due to the less strain of a seven-member ring formation in this than a usual five or six member ring formation [36].

ESI mass spectra provide evidence of the formation of a 1:1 **1**–Hg^{2+} complex in 50 % CH_3CN/CH_2Cl_2 solution (Fig. S13). The peak at m/z=902.3 (calcd. 902.3), corresponding to $[(\mathbf{1}\text{-H}) + Hg + CH_3CN - NO]^{+}$, is observed when $HgCl_2$ (36 μmol) is added to **1** (30 μmol), whereas free **1** exhibits a peak at m/z=691.3, which corresponds to $[\mathbf{1}+H]^{+}$ (Fig. S3 in Supplementary data). As the usual coordination number of Hg (II) is four, anion Cl^{-} may be the counteranion of **1**-Hg^{2+}, as indicated in Scheme 2. Ratiometric fluorescent Zn^{2+} and Cu^{2+} chemosensors based on deprotonation of secondary amines were reported in the literatures [36–39].

Fig. 7 Color changes of compound **1** (20 μM) on addition of different metal ions (80 μM) in ethanol/aqueous tris buffer (9:1, v/v) of pH 9.17. From left to right: blank, Hg^{2+}, Zn^{2+}, Cd^{2+}, Mn^{2+}, Co^{2+}, Ni^{2+}, Cr^{3+}, Fe^{3+}, Cu^{2+}, Pb^{2+}, Ag^{+}

The variation of the two fluorescence intensities affords the system a ratiometric sensor for mercury ions in aqueous ethanol solutions under neutral to basic conditions; and such a ratiometric sensing system for Hg^{2+} ions possesses two advantages, one is a large wavelength shift (100 nm) between the excitation peak and emission peak, which eliminates the influence of excitation backscattering effects on the fluorescence assay; the other is the presence of two well-resolved emission peaks with comparable fluorescence intensities, which ensures high resolution for the ratiometric sensing.

Selectivity Investigation

The fluorescence responses of probe **1** to various cations in ethanol/aqueous tris buffer (9:1, v/v) of pH 9.17 and its selectivity for Hg^{2+} are explored. The concentration of Hg^{2+} was fixed at 2×10^{-5} mol L^{-1}. The fluorescence spectrum of probe **1** was bathochromically shifted with increased intensity in the presence of Hg^{2+}. However, the fluorescence intensity and maxima of probe **1** remained unchanged upon addition of other cations (Fig. S14, Supplementary material). I_{569}/I_{529} was significantly enhanced upon the addition of Hg^{2+} (purple bars in Fig. 6). However, the addition of other cations did not affect I_{569}/I_{529} of the fluorescent probe **1**. In order to further test the interference for other cations on the determination of Hg^{2+}, a competition experiment was performed in which the fluorescent probe was added to a solution of Hg^{2+} in the presence of other metal ions (red bars in Fig. 6). The competition experiments show slight variation in the emission intensity ratio (I_{569}/I_{529}) except Cr^{3+} and Fe^{3+}. Thus, probe **1** exhibits a good selectivity for Hg^{2+} over the tested metal ions except Cr^{3+} and Fe^{3+}. Additionally, to explore the effects of anionic counterions on the sensing behavior of **1** to metal ions, absorption responses of **1** to mercury nitrate were examined (Fig. S15, Supplementary material). The results were similar to that shown in Fig. 3. There were no obvious changes in the absorption responses of **1** to $HgCl_2$, and $Hg(NO_3)_2$. Color changes of compound **1** upon addition of 2 equivalents of Hg^{2+} were obviously different from no addition or addition of other ions (Fig. 7). The color change from yellow to red of **1** facilitated naked-eye recognition of Hg^{2+} under neutral to basic conditions.

Conclusions

In summary, a new probe based on a nitrobenzoxadiazolyl (NBD) liked with a spirolactam rhodamine derivative by diethylenetriamine was reported. It exhibits good selectivity with ratiometric response for Hg^{2+} in aqueous ethanol solutions under neutral to basic conditions based on deprotonation of -NH- conjugated to NBD process and ICT mechanism. It shows nanomolar affinity and shows large fluorescent shifts and enhancement. The colorimetric response with a large red-shift emission was useful for the easy detection of Hg^{2+}.

Acknowledgments The authors thank the NSFC (project No. 21102037 and 21201057) and the Education Department of Henan Province (No. 2010GGJS-048) for the financial support.

References

1. de Silva AP, Gunaratne HQN, Gunnlaugsson T, Huxley AJM, McCoy CP, Rademacher JT, Rice TE (1997) Signaling recognition events with fluorescent sensors and switches. Chem Rev 97:1515–1566
2. Patrick L (2002) Mercury toxicity and antioxidants. Part 1. Role of glutathione and alpha-lipoic acid in the treatment of mercury toxicity. Altern Med Rev 7:456–471
3. Grandjean P, Weihe P, White RF, Debes F (1998) Cognitive performance of children prenatally exposed to "safe" levels of methylmercury. Environ Res 77:165–172
4. Harada M (1995) Minamata disease: methylmercury poisoning in Japan caused by environmental pollution. Crit Rev Toxicol 25:1–25
5. Han J, Burgess K (2010) Fluorescent indicators for intracellular pH. Chem Rev 110:2709–2728
6. Quang DT, Kim JS (2010) Fluoro- and chromogenic chemodosimeters for heavy metal ion detection in solution and biospecimens. Chem Rev 110:6280–6301
7. Coskun A, Akkaya EU (2006) Signal ratio amplification via modulation of resonance energy transfer: proof of principle in an emission ratiometric Hg(II) sensor. J Am Chem Soc 128:14474–14475
8. Lin W, Yuan L, Long L, Guo C, Feng J (2008) A fluorescent cobalt probe with a large ratiometric fluorescence response via modulation of energy acceptor molar absorptivity on metal ion binding. Adv Funct Mater 18:2366–2372
9. Zhang X, Xiao Y, Qian X (2008) A ratiometric fluorescent probe based on FRET for imaging Hg^{2+} ions in living cells. Angew Chem Int Ed 47(42):8025–8029
10. Shang G-Q, Gao X, Chen M-X, Zheng H, Xu J-G (2008) A novel Hg^{2+} selective ratiometric fluorescent chemodosimeter based on an intramolecular FRET mechanism. J Fluoresc 18(6):1187–1192
11. Han Z-X, Luo H-Y, Zhang X-B, Kong R-M, Shen G-L, Yu R-Q (2009) A ratiometric fluorescent chemosensor for fluorescent determination of Hg^{2+} based on a new porphyrin-quinoline dyad. Spectrochim Acta A 72A(5):1084–1088
12. Mahapatra AK, Hazra G, Das NK, Sahoo P, Goswami S, Fun H-K (2011) A highly sensitive and selective ratiometric fluorescent probe based on conjugated donor-acceptor-donor constitution of 1,8-naphthyridine for Hg^{2+}. J Photochem Photobiol A 222(1):47–51
13. Wang J, Zhang L, Qi Q, Li S, Jiang Y (2013) Specific ratiometric fluorescent sensing of Hg^{2+} via the formation of mercury(II) barbiturate coordination polymers. Anal Methods 5(3):608–611
14. Liu J, Sun Y-Q, Wang P, Zhang J, Guo W (2013) Construction of NIR and ratiometric fluorescent probe for Hg^{2+} based on a rhodamine-inspired dye platform. Analyst 138(9):2654–2660
15. Liu B, Zeng F, Wu G, Wu S (2011) A FRET-based ratiometric sensor for mercury ions in water with multi-layered silica nanoparticles as the scaffold. Chem Commun 47:8913–8915
16. Liu B, Zeng F, Wu G, Wu S, Wang J, Tang F (2013) Ratiometric sensing of mercury(II) based on a FRET process on silica core-shell nanoparticles acting as vehicles. Microchim Acta 180:845–853
17. Lakowicz JR (1994) Topics in fluorescence spectroscopy. In: Probe design and chemical sensing, vol 4. Plenum Press, New York

18. Grabowski ZR, Rotkiewicz K (2003) Structural changes accompanying intramolecular electron transfer: focus on twisted intramolecular charge-transfer states and structures. Chem Rev 103:3899–4032
19. Kiyose K, Kojima H, Urano Y, Nagano T (2006) Development of a ratiometric fluorescent zinc ion probe in near-infrared region, based on tricarbocyanine chromophore. J Am Chem Soc 128:6548–6549
20. Cotton FA, Wilkinson G (1980) Advanced inorganic chemistry, 4th edn. John Wiley & Sons, New York
21. Liu Y, Zhang N, Chen Y, Wang LH (2007) Fluorescence sensing and binding behavior of aminobenzenesulfonamidoquinolino-β-cyclodextrin to Zn^{2+}. Org Lett 9:315–318
22. Uchiyama S, Santa T, Imai K (1999) Fluorescence characteristics of six 4,7-disubstituted benzofurazan compounds: an experimental and semi-empirical MO study. J Chem Soc Perkin Trans 2:2525–2532
23. Ramachandram B, Samanta A (1998) Transition metal ion induced fluorescence enhancement of 4-(N, N-dimethylethylenediamino)-7-nitrobenz-2-oxa-1,3-diazole. J Phys Chem A 102:10579–10587
24. Guminskia Y, Grousseaud M, Cugnasse S, Brel V, Annereaub JP, Visp S, Guilbaud N, Barret JM, Bailly C, Imbert T (2009) Synthesis of conjugated spermine derivatives with 7-nitrobenzoxadiazole (NBD), rhodamine and bodipy as new fluorescent probes for the polyamine transport system. Bioorg Med Chem Lett 19:2474–2477
25. Charier S, Ruel O, Baudin JB, Alcor D, Allemand JF, Meglio A, Jullien L (2004) An efficient fluorescent probe for ratiometric pH measurements in aqueous solutions. Angew Chem Int Ed 43:4785–4788
26. Onoda M, Uchiyama S, Santa T, Imai K (2002) The effects of spacer length on the fluorescence quantum yields of the benzofurazan compounds bearing a donor–acceptor system. Luminescence 17:11–14
27. Bem M, Badea F, Draghici C, Caproiu MT, Vasilescu M, Voicescu M, Beteringhe A, Caragheorgheopol A, Maganu M, Constantinescu T, Balaban AT (2007) Synthesis and fluorescent properties of new derivatives of 4-amino-7-nitrobenzofurazan. Arkivoc 2007(xiii):87–104
28. Zhang X, Shiraishi Y, Hirai T (2007) Cu(II)-selective green fluorescence of a rhodamine−diacetic acid conjugate. Org Lett 9:5039–5042
29. Anthoni U, Christophersen C, Nielsen P, Puschl A, Schaumburg K (1995) Structure of red and orange fluorescein. Struct Chem 6: 161–165
30. Czarnik AW (1993) Fluorescent chemosensor for ion and molecule recognition. American Chemical Society, Washington, DC
31. Bag B, Bharadwaj PK (2004) Attachment of an electron-withdrawing fluorophore to a cryptand for modulation of fluorescence signaling. Inorg Chem 43:4626–4630
32. Uchiyama S, Takehira K, Kohtani S, Imai K, Nakagaki R, Tobita S, Santa T (2003) Fluorescence on–off switching mechanism of benzofurazans. Org Biomol Chem 1:1067–1072
33. Filik H, Hayvali M, Kilic E (2005) Sequential spectrophotometric determination of paracetamol and p-aminophenol with 2,2′-(1,4-phenylenedivinylene) bis-8-hydroxyquinoline as a novel coupling reagent after microwave assisted hydrolysis. Anal Chim Acta 535: 177–182
34. Li ZF, Xiang Y, Tong AJ (2008) Ratiometric chemosensor for fluorescent determination of Zn^{2+} in aqueous ethanol. Anal Chim Acta 619:75–80
35. Valeur B, Leray I (2000) Design principles of fluorescent molecular sensors for cation recognition. Coord Chem Rev 205:3–40
36. Xu Z, Qian X, Cui J, Zhang R (2006) Exploiting the deprotonation mechanism for the design of ratiometric and colorimetric Zn^{2+} fluorescent chemosensor with a large red-shift in emission. Tetrahedron 62:10117–10122
37. Du J, Fan J, Peng X, Li H, Sun S (2010) The quinoline derivative of ratiometric and sensitive fluorescent zinc probe based on deprotonation. Sensors Actuators B 144:337–341
38. Xu Z, Qian X, Cui J (2005) Colorimetric and ratiometric fluorescent chemosensor with a large red-shift in emission: Cu(II)-only sensing by deprotonation of secondary amines as receptor conjugated to naphthalimide fluorophore. Org Lett 7(14):3029–3032
39. Kaur N, Kumar S (2008) Near-IR region absorbing 1,4-diaminoanthracene-9,10-dione motif based ratiometric chemosensors for Cu^{2+}. Tetrahedron 64:3168–3175